BIOCHEMISTRY
including biophysical chemistry & molecular biology

Article

pubs.acs.org/biochemistry

Flexible Docking-Based Molecular Dynamics/Steered Molecular Dynamics Calculations of Protein−Protein Contacts in a Complex of Cytochrome P450 1A2 with Cytochrome b_5

Petr Jeřábek,[†] Jan Florián,[§] Marie Stiborová,[†] and Václav Martínek*[,†,‡]

[†]Department of Biochemistry, Faculty of Science, Charles University in Prague, Albertov 2030, 128 43 Prague 2, Czech Republic

[‡]Department of Teaching and Didactics of Chemistry, Faculty of Science, Charles University in Prague, Albertov 3, 128 43 Prague 2, Czech Republic

[§]Department of Chemistry and Biochemistry, Loyola University Chicago, 1032 West Sheridan Road, Chicago, Illinois 60660, United States

Supporting Information

ABSTRACT: Formation of transient complexes of cytochrome P450 (P450) with another protein of the endoplasmic reticulum membrane, cytochrome b_5 (cyt b_5), dictates the catalytic activities of several P450s. Therefore, we examined formation and binding modes of the complex of human P450 1A2 with cyt b_5. Docking of soluble domains of these proteins was performed using an information-driven flexible docking approach implemented in HADDOCK. Stabilities of the five unique binding modes of the P450 1A2−cyt b_5 complex yielded by HADDOCK were evaluated using explicit 10 ns molecular dynamics (MD) simulations in aqueous solution. Further, steered MD was used to compare the stability of the individual P450 1A2−cyt b_5 binding modes. The best binding mode was characterized by a T-shaped mutual orientation of the porphyrin rings and a 10.7 Å distance between the two redox centers, thus satisfying the condition for a fast electron transfer. Mutagenesis studies and chemical cross-linking, which, in the absence of crystal structures, were previously used to deduce specific P450−cyt b_5 interactions, indicated that the negatively charged convex surface of cyt b_5 binds to the positively charged concave surface of P450. Our simulations further elaborate structural details of this interface, including nine ion pairs between R95, R100, R138, R362, K442, K455, and K465 side chains of P450 1A2 and E42, E43, E49, D65, D71, and heme propionates of cyt b_5. The universal heme-centric system of internal coordinates was proposed to facilitate consistent classification of the orientation of the two porphyrins in any protein complex.

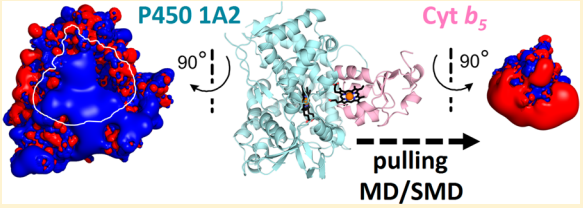

Cytochrome P450 enzymes (P450s) are hemoproteins, which represent a large, versatile, and important superfamily of naturally occurring monooxygenases.[1] These enzymes employ two electrons, two protons, and molecular oxygen to oxidize a wide variety of organic compounds of different structure and size such as drugs, steroids, and carcinogens. Eukaryotic P450s are usually located in the membrane of the endoplasmic reticulum. Cytochrome b_5 (cyt b_5), another hemoprotein of the endoplasmic reticulum membrane, has been shown to modulate P450-dependent reactions *in vitro*.[2,3] Experiments utilizing mice with the conditional deletion of microsomal cyt b_5 in liver showed that cyt b_5 also plays an important role in the function of hepatic P450s *in vivo*.[2] Furthermore, experiments with complete null mice have shown that deletion of microsomal cyt b_5 in all organs strongly affects hepatic and extrahepatic drug metabolism and testicular P450 17A1 hydroxylase/lyase activities.[4]

The P450−cyt b_5 complex forms spontaneously. In particular, P450 1A2−cyt b_5 and P450 2B4−cyt b_5 heterodimers were observed in experiments utilizing rabbit liver microsomes and soluble carbodiimide.[5] Cyt b_5 may enhance, may inhibit, or has no effect on catalysis by microsomal P450s, depending on the particular P450 isoform, the substrate, and the experimental conditions.[6,7] Several studies have suggested mechanisms by which cyt b_5 could stimulate P450 reactions,[8] including the cyt b_5-mediated transfer of the second electron to P450 that occurs faster than through NADPH:P450 oxidoreductase.[9−11] Alternatively, cyt b_5 may stimulate P450 via an allosteric mechanism without direct participation of an electron transfer.[10,12,13] This hypothesis is consistent with the results of studies employing cyt b_5 lacking the heme cofactor (apo-cyt b_5)[13−15] or containing the Mn-protoporphyrin IX instead of heme.[6,16] The participation of the allosteric mechanism is also supported by a recently reported cyt b_5-mediated increase in P450 efficiency through improving reaction coupling efficiency.[3]

The functional outcomes of P450−cyt b_5 interactions depend strongly on the reaction, substrate, and the P450 type. Reactions catalyzed by P450s of the 2A, 2B, 2C, 2E, and 3A subfamilies are usually stimulated by the presence of cyt b_5, the 3A subfamily being the most sensitive,[12,14] but the excess of cyt b_5 may inhibit

Received: July 2, 2014
Revised: September 4, 2014
Published: October 14, 2014

ACS Publications © 2014 American Chemical Society

P450 2B6[17] and P450 2B4.[16] Oxidation of marker substrates of P450 1A1, 1A2, 1B1, and 2D6 is insensitive to cyt b_5.[13] However, the P450 1A1- and P450 1A2-mediated oxidation of several nonmarker substrates, including Sudan I[17] and aristolochic acid I,[18] is stimulated by cyt b_5. Notably, the holo-cyt b_5 considerably alters the ratio of ellipticine metabolites formed by P450 1A1, 1A2, and 3A4 reconstituted with NADPH:P450 oxidoreductase, thus favoring formation of reactive metabolites 12-hydroxy- and 13-hydroxyellipticine at the expense of detoxication products, 9-hydroxy- and 7-hydroxyellipticine. This change in a metabolite ratio results in an increased degree of formation of covalent ellipticine−DNA adducts. Therefore, cyt b_5 is shifting ellipticine detoxication to activation.[19−21]

Interprotein contacts in complexes of cyt b_5 with P450s were studied using site-directed mutagenesis, nuclear magnetic resonance (NMR) spectroscopy, and cross-linking experiments.[3,22−24] Several residues located on a proximal surface of P450 2B4[23,25] and P450 2E1[26,27] were identified to be involved in interactions with cyt b_5. Therefore, it is generally accepted that the convex and acidic surface of cyt b_5 binds to the basic concave surface of a P450 protein.[28] Binding affinities between microsomal proteins, including several P450s and cyt b_5, were also determined in immobilized systems.[29] However, no three-dimensional structure of the P450−cyt b_5 complex has been determined by experimental methods.[30]

In this paper, we examine interactions of human cyt b_5 with P450 1A2 using various methods of computational chemistry. The P450 enzymes of the 1A subfamily play a major role in the activation of various planar hydrophobic xenobiotics, such as benzo[*a*]pyrene and other polycyclic aromatic hydrocarbons, aromatic and heterocyclic amines, azo dyes like dimethylaminoazobenzene or Sudan I, and several drugs such as ellipticine.[19−21,31−39]

It was estimated that the human interactome contains ∼130000 binary protein−protein interactions, most of them remaining to be mapped.[40] Protein−protein docking is a widely used technique for prediction of these complexes. However, exploring the entire protein surface is computationally very demanding. Thus, experimental data can be employed to constrain the search to certain areas of protein surfaces.[41] Such constraints can significantly decrease computational time as demonstrated by the improved performance of HADDOCK during the CAPRI (Critical Assessment of PRediction of Interactions) competition.[42,43] The docking methods had shown a potential to predict a structure of strong, permanent protein−protein complexes, e.g., in a CAPRI blind test competition. However, similar predictions become more challenging for transient protein complexes, such as those between proteins involved in the electron transfer.[44,45] To expand the conformational space of the explicit solvent molecules and related protein−solvent interactions, we refined and reevaluated structures of complexes obtained from docking using classical all-atom molecular dynamics (MD).

Docking methods combined with experimental constrains were recently used for prediction of P450 2B4−cyt b_5 complexes.[22,24] However, the results obtained from these docking methods were rather ambiguous, predicting more than one structure of the resulting complex. Accurate discrimination among several possible binding modes represents another challenging issue for computer simulation. The best discriminator would be the binding free energy calculated using rigorous all-atom methods like free energy perturbation, linear response approximation, or linear interaction energy.[41,46−49] However, these methods are currently not suitable for predicting the stability of protein−protein complexes, because of their large sampling requirements, and are limited only to smaller ligand molecules. Thus, in this study, we also evaluated the external work performed during dissociation of protein complexes using the steered molecular dynamics (SMD) calculations in implicit solvent. The performance of these and related algorithms for free energy prediction has been recently investigated.[50−53] Interestingly, of the several possible cyt b_5−P450 complexes predicted by protein−protein docking (Figure 1), both our MD and SMD

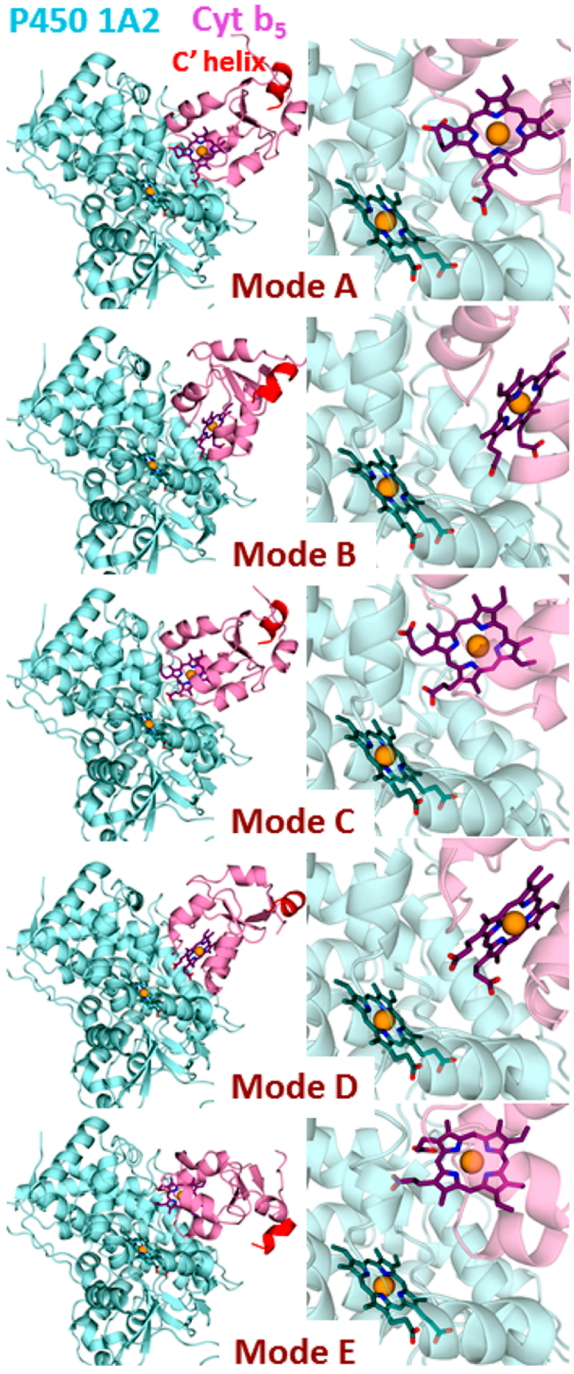

Figure 1. Studied P450 1A2−cyt b_5 complexes (left, overall view; right, detail of the heme moieties). Cyt b_5, P450 1A2, heme cofactors, and ferric ions are represented by pink and cyan colors, sticks, and yellow spheres, respectively.

dx.doi.org/10.1021/bi500814t | *Biochemistry* 2014, 53, 6695−6705

simulations identified the same binding mode to be the most stable, thus suggesting that this mode represents the possible binding mode of the human P450 1A2–cyt b_5 complex.

METHODS

Structures of Individual Proteins. The initial coordinates of truncated human P450 1A2, which were used in our docking simulations, were based on X-ray structural data (PDB entry 2HI4).[54] For cyt b_5, there are several three-dimensional structures deposited in the PDB, but only one of them contains the human microsomal protein. Because this structure, which is based on NMR restraints (PDB entry 2I96),[55] is lacking the last helix in the C-terminal region, we used server SWISS-MODEL[56] to construct a homologous model of human cyt b_5 based on an X-ray structure of bovine cyt b_5 (PDB entry 1CYO).[57] Because the soluble domain of bovine cyt b_5 differs from its human ortholog only in five surface amino acid residues, thus showing 94% sequence identity and 99% homology (Figure S1 of the Supporting Information), our human cyt b_5 model is likely to be reasonably accurate.

Protein–Protein Docking. *In silico* protein–protein docking of truncated human P450 1A2 and the soluble domain of human cyt b_5 was performed using a flexible docking protocol implemented in HADDOCK.[43] HADDOCK utilizes known structural elements in a protein interface to generate proximity restraints that are employed to guide the docking process. In particular, a structure that is generated during the course of docking is penalized by lowering its score when the predefined "active" residues are not participating in protein–protein contacts. Residues predefined as "passive" are positioned close to the other protein when the simulation starts, but no penalty is imposed later, if a passive residue moves away from the protein–protein interface.

We conducted 11 docking calculations using various combinations of active and passive residues. Their selection was based on the results of experimental studies of the P450 2B4–cyt b_5 interactions[3,22,23] and a structural alignment of the P450 1A2 and P450 2B4 proteins. These two P450s show poor sequence similarity; however, they have good structural homology (rmsd = 1.6 Å). Several docking setups also considered one or both heme cofactors to be in the proximity of the binding interface (Table 1 and Figure S2 of the Supporting Information).

Heme-centric Internal Coordinate System. The mutual orientation of heme cofactors of P450 1A2 and cyt b_5 was expressed in terms of spherical coordinates and Euler angles; the VMD/Tcl script calculating these parameters is provided in the Supporting Information. Spherical coordinates (r, ϕ, θ) were used to describe the spatial position of the Fe atom of cyt b_5 in the coordinate system centered at the P450 1A2 heme, whereas the cyt b_5 heme rotation was specified using Euler angles (α, β, γ) (Figure 2). A similar coordinate system has been applied to study the effect of microwave-excited rotational motion of polar molecules on their chemical reactivity[58,59] and solvation properties.[60]

MD and SMD Calculations. Geometries of five binding modes obtained from protein–protein docking were used as starting geometries for MD and SMD simulations. Hydrogen atoms and protonation states of histidine residues corresponding to neutral pH were assigned using WHATIF.[61] All water molecules present in the original PDB files were preserved except for waters located at the interface of both proteins. The system was then solvated using Solvate version 1.0[62] and placed in a TIP3P water box with >15 Å margins using VMD version 1.9.1.[63] The overall charge of the solute was neutralized by adding two

Table 1. Summary of Active and Passive Residues Used as Restrains for Individual Protein–Protein Docking Runs

	human cytochrome P450 1A2		human cytochrome b_5		
docking setup	active residue	passive residue	active residue	passive residue	source[b]
1	T146, R281, E446, E461	auto[a]	none	all charged	22
2	heme	auto[a]	heme	auto[a]	*ab initio*
3	R138, K455	heme	D65, V66	heme	3
4	R138, K455, heme	auto	D65, V66, heme	auto[a]	3
5	R138, F147, K455	heme	D65, V66	heme	3, 23
6	R138, F147, K455, heme	auto	D65, V66, heme	auto[a]	3, 23
7	R138, F147, K455	heme	D65, V66	all charged	3, 23
8	R138, F147, K455, heme	auto[a]	heme	all charged	23
9	R138, K455	heme	heme	all charged	23
10	heme	R138, K455	heme	all charged	23
11	R138, K455, heme	auto[a]	none	all charged	23

[a]All surface residues lying within a 6.5 Å radius of each active residue were selected automatically. [b]Active residues were chosen to be analogous to those identified by experimental studies of P450 2B4. "*ab initio*" means no experimental data were used during docking.

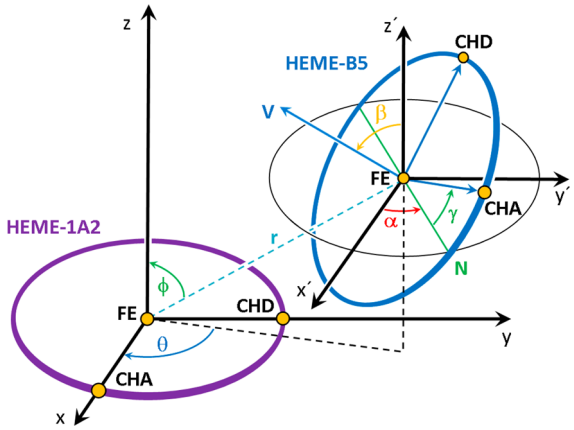

Figure 2. Schematic outline of geometric parameters describing the mutual orientation of two heme molecules. The porphyrin cycle of the heme molecule of P450 1A2 (HEME-1A2) is represented as a purple circle. This cycle is oriented in a way that the Fe^{3+} ion is placed in the origin of the coordinate system; a vector connecting Fe and CHA atoms is oriented along the x-axis and the vector connecting Fe and CHD atoms along the y-axis. Axes x', y', z' are chosen to be parallel with x, y, z, respectively. The spatial position of the Fe atom of the heme molecule of cytochrome b_5 (HEME-B5, blue circle) is described using spherical coordinates (r, ϕ, θ). The rotation of this heme is described by Euler angles α, β, and γ. The N-axis (green) is defined as the intersection of the x–y plane (black circle) and the plane of HEME-B5. α is an angle between the x'-axis and the N-axis. Vector **V** originates in the HEME-B5 Fe atom and is perpendicular to the heme plane. β is an angle between vector **V** and the z'-axis (two porphyrin cycles are parallel if β is 0° or 180° and perpendicular if β is 90° or 270°). γ is defined as the angle between the N-axis and the vector connecting the Fe and CHA atoms; a change in this angle shows rotation of the heme plane about vector **V**.

dx.doi.org/10.1021/bi500814t | *Biochemistry* 2014, 53, 6695–6705

Table 2. Clustering of Results from Protein−Protein Docking of P450 1A2 and Cyt b_5 (overall scores, contact surfaces, and electron transfer distances)

binding mode (Figure 1)	HADDOCK score (kcal/mol)[b]	buried surface area (Å^2)[b]	distance between redox centers (r_{da}) (Å)[c]	parameters describing mutual orientation of heme molecules[d]					
				r (Å)	ϕ (deg)	θ^e (deg)	α (deg)	β (deg)	γ (deg)
mode A									
3	−152 ± 8	1506 ± 170	10.7	17.3	9	27	37	97	87
4a	−170 ± 7	1648 ± 30	10.4	17.0	3	61	43	89	99
5	−139 ± 17	1573 ± 210	10.0	16.5	7	6	34	92	94
6	−172 ± 5	1766 ± 100	10.6	17.0	1	178	48	90	103
7	−152 ± 4	1578 ± 100	10.4	16.8	10	22	47	95	95
8a[a]	−166 ± 9	1650 ± 150	9.8	16.3	6	7	55	95	90
10	−164 ± 15	1563 ± 190	10.7	17.2	6	41	39	93	105
mode B									
4b[a]	−169 ± 9	1687 ± 30	10.6	17.1	11	46	97	104	119
9	−152 ± 18	1560 ± 150	10.9	17.5	16	60	96	101	121
mode C									
2[a]	−187 ± 10	1716 ± 160	9.1	15.6	7	186	49	92	103
11	−169 ± 10	1550 ± 70	9.4	16.3	2	213	43	91	123
mode D									
8b[a]	−158 ± 22	1561 ± 120	12.5	19.0	12	319	92	94	62
mode E									
1[a]	−188 ± 2	1946 ± 70	10.7	17.4	5	211	5	49	124

[a]The complex with the shortest electron donor−acceptor distance was used as the cluster representative (Figure 1). [b]Data represent the means ± standard deviations of the cluster calculated by HADDOCK. [c]Distance between heme prosthetic groups of P450 1A2 and cyt b_5. [d]For the definition of individual geometrical parameters, see Figure 2. [e]The θ value becomes redundant when angle ϕ approaches 0°.

Cl^- ions; 26 additional K^+ ions and 26 additional Cl^- ions were uniformly distributed in the solvent to mimic a 0.1 M KCl solution. Every protein complex was equilibrated prior to the production run in six subsequent steps (Table S1 of the Supporting Information).

Production phase MD calculations were conducted in explicit solvent under periodic boundary conditions in the *NPT* ensemble (310 K, 1 atm). The temperature and pressure were held constant using Langevin dynamics (friction coefficient 1) and the Langevin piston method implemented in NAMD version 2.9.[64] All MD and SMD simulations were conducted with 2 and 1 fs time steps, respectively. The cutoff for short-range interactions was 12 Å. For electrostatic (ES) interactions, we used the particle mesh Ewald method[65] implemented in NAMD. Bonds involving hydrogen atoms and TIP3P water were kept rigid using the SHAKE algorithm.[66] All simulations were performed with the CHARMM27 force field.[67] The simulated system was relatively large (approximately 100 Å × 100 Å × 100 Å) and contained ∼100000 atoms, but we made use of advances in implementation of a GPU accelerated code[68] in NAMD version 2.9, resulting in substantial acceleration (5−10 times).

To evaluate the stability of an individual binding mode, backbone atoms of P450 1A2 were aligned with their initial positions in a docking complex. For each complex that was aligned in this way, the rmsd of the cyt b_5 backbone from its initial geometry was examined along the MD trajectory. The formation of hydrogen bonds was monitored using VMD (hydrogen bond plug-in) with a 3 Å cutoff distance and a 20° cutoff angle. We also monitored the electron donor−acceptor distance (r_{da}) as the shortest distance between the two redox centers (i.e., heme porphyrins). Because the two hemes adopt a nearly T-shaped geometry in all studied complexes (Figure 1), this distance was approximated as the Fe−Fe distance minus the sum of the porphyrin disk radius (4.2 Å) and the Fe−S bond distance (2.32 Å).

The inputs for SMD calculations were prepared akin to MD inputs, except that, an implicit solvent and the constant velocity protocol[69] were applied to enforce pulling of cyt b_5 from P450 1A2. The force constant (100 kcal mol^{-1} Å^{-2})[70] was applied to the cyt b_5 center of mass. The cyt b_5 center was pulled away from P450 1A2 at a speed of 20 Å/ns. The results of SMD calculations were shown to be insensitive to the pulling direction;[71] thus, the cyt b_5 was pulled in a direction perpendicular from P450 1A2 (dashed arrow in Figure 5), resulting in the shortest dissociation path. C_α atoms of P450 1A2 were fixed during the SMD simulations at their starting coordinates to prevent the overall translation of the system. The Cartesian coordinates of C_α atoms of cyt b_5 were constrained inside the plane that was perpendicular to the pulling direction by weak force constant of 0.05 kcal mol^{-1} Å^{-2} to prevent cyt b_5 from rolling on the surface of P450. The dissociation free energy was assumed to be proportional to the difference between the average work for the last 3 Å of the dissociation path and the minimal value of the calculated work, which usually occurred within first 1 Å of the pulling process. The dissociation of each complex was conducted in three parallel simulations with different seed numbers. The average external work necessary for translation of the cyt b_5 center of mass in a system lacking P450 1A2 was subtracted to compensate for effects not related to interaction between cyt b_5 and P450 1A2 proteins.

To visualize ES properties of studied proteins, we used the Adaptive Poisson−Boltzmann Solver (APBS)[72] plug-in of PyMOL.[73] Atom radii and charges were consistent with the CHARMM27 force field used here. An effect of the solvent on the resulting ES field was mimicked using a monovalent ion concentration of 0.15 M and variable dielectric constants of 2.0 and 78.0 for the protein and solvent, respectively. The ES

dx.doi.org/10.1021/bi500814t | *Biochemistry* 2014, 53, 6695−6705

potentials of individual studied proteins were displayed as positive/negative isosurface with the isovalue set to +2 k_BT/e for the positive potential and −2 k_BT/e for the negative one.

RESULTS

Clustering of the Docked Complexes. A flexible protein−protein docking method was employed to obtain a set of plausible orientations of water-soluble domains of both cytochromes. The flexible treatment of both proteins during the docking procedure allowed induction of limited structural changes of a protein imposed by the presence of its interacting partner. We docked cyt b_5 to P450 1A2 using 11 different input parameter sets, including (i) amino acid residues analogous to those found to be important for interactions of P450 with cyt b_5 (mutational studies) or (ii) residues of related proteins labeled by cross-linking reagents (Table 1 and references cited therein).

From 3300 structures evaluated during 11 docking runs, we obtained 13 clusters of protein complexes that were characterized by the best docking score, a large buried surface area, and a small distance between heme cofactors. Despite the differences in input parameters, most docking runs predicted structurally related complexes. These similar binary complexes were identified and regrouped, using heme-centric coordinates (Table 2) and the rmsd matrix (Table S2 of the Supporting Information), into five superclusters representing structurally distinctive binding modes A−E (Figure 1). The complex with the shortest electron donor−acceptor distance was selected as the cluster representative. The relative orientation of the two proteins, represented as mutual orientation of their heme cofactors, is specified in Table 2. A schematic outline of six geometrical parameters introduced here for mutual orientation of heme cofactors is shown in Figure 2. We prefer these coordinates to, e.g., Cartesian coordinates because the spherical parameter r and the angle β can be directly interpreted as the Fe−Fe distance and the inclination of heme planes, respectively. Parameters r and ϕ illustrate that the Fe atom of cyt b_5 is in all binding modes found in the proximity and also that it is positioned almost directly above the heme of P450 1A2. All binding modes show similar relative position of their Fe atoms, but they differ in the relative rotation of cyt b_5. This is demonstrated in the variation of geometrical parameters α, β, and γ (Table 2).

Binding mode A was the most populated among our docked structures, but the HADDOCK score and the contact interface area favored mode E. Because the binding mode representing the most stable complex could not be unambiguously identified via docking calculations, all binding modes were further examined using MD simulations.

Dynamical Properties of the P450 1A2−Cyt b_5 Complexes. The geometry of each binding mode (Figure 1, modes A−E) was refined using a 10 ns MD simulation at 310 K in the explicit water environment. While the potential energy declined during these simulations (Figure 3A), energies of modes A and D reached reasonable convergence near 8 ns. However, only the geometry of mode A was sufficiently stable throughout the whole simulation, as illustrated by a small root-mean-square deviation (rmsd) of the cyt b_5 backbone atoms, fluctuating only up to 3 Å from its initial docked position (Figure 3B). This is consistent with the normal dynamic motion of the cyt b_5 protein.

A 14 Å electron donor−acceptor distance (r_{da}) is sufficient to facilitate efficient electron transfer between the two redox centers embedded in a protein medium.[74] When r_{da} is defined as the edge-to-edge distance between redox centers of P450 1A2 and cyt b_5 (Figure 3C), only binding mode A, in which r_{da} fluctuates between 10.4 and 10.7 Å, permits facile electron transfer. On the other hand, modes B−E become dissociated during the course of the MD simulations, all ending with r_{da} distances between 13.7 and 15 Å.

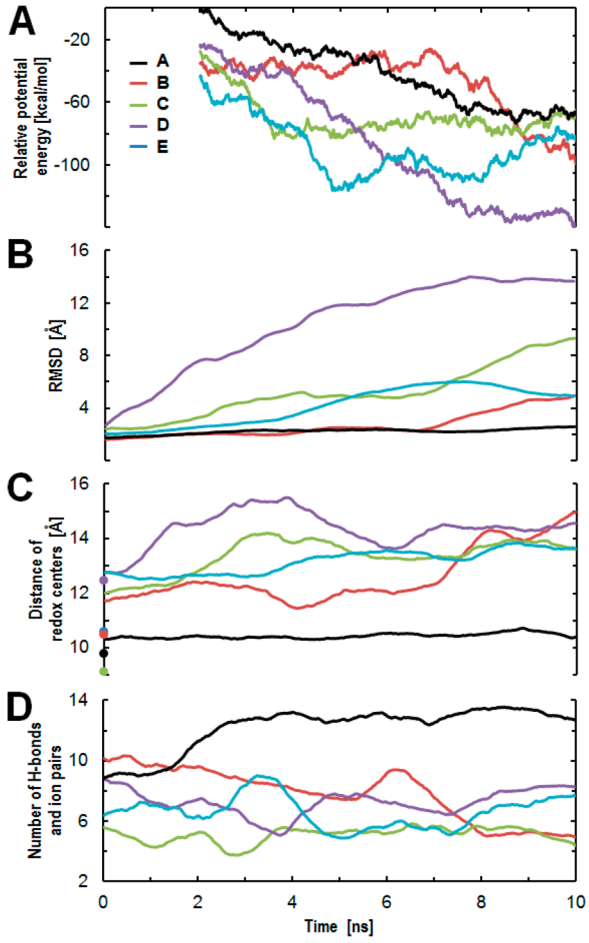

Figure 3. Dynamical properties of P450 1A2−cyt b_5 complexes during an unconstrained MD simulation. Average relative potential energies (A), rmsd of cyt b_5 (B), distances between redox centers (C), and interprotein hydrogen bonding and ion pairing (D) of all five P450 1A2−cyt b_5 binding modes were plotted vs time. Initial distances between redox centers are shown as colored circles. For a more detailed definition of the rmsd and distances, see Methods: black for mode A, red for mode B, green for mode C, purple for mode D, and blue for mode E.

The contact interface of transient protein−protein complexes, unlike the permanent protein−protein complexes, is more plastic and less sensitive to mutations.[75] Transient complexes also contain, on average, more hydrophilic residues in their interfaces than the permanent complexes.[76,77] Therefore, it seems that not only hydrophobic interactions but also ES complementarity and hydrogen bonding are contributing to the stabilization of transient protein−protein complexes. ES interactions, however, are insufficiently optimized during a typical docking procedure. All complexes obtained from the docking showed between five and nine interprotein ES contacts (ion pairs and hydrogen bonds), but more rigorous treatment of hydrogen bonding across the entire system should verify their stability.[47,78] Figure 3D shows the development of ES contacts between P450 1A2 and cyt b_5 during unconstrained MD simulations of all binding modes evaluated here. Of the interprotein hydrogen bonds of modes A−E, only those in mode A were substantially improved during its

dx.doi.org/10.1021/bi500814t | Biochemistry 2014, 53, 6695−6705

MD relaxation as its number of interprotein ES contacts increased from 7 to 12.

Complex Dissociation. To study the feasibility of the dissociation of heterodimers in binding modes A−E, we slowly pulled the two proteins approximately 15 Å apart using the SMD method. The pulling speed of 20 Å/ns used here is relatively high and results in a nonequilibrium dissociation process. Therefore, the external work done during this simulation significantly overestimates the dissociation free energy. Although the energy for the reversible thermodynamic process cloud be obtained using the Jarzynski equality,[79] it would require hundreds of parallel simulations and also a much slower pulling speed to keep the standard deviation of the work distributions comparable to k_BT.[71,80] Thus, to compare stabilities of the individual P450 1A2−cyt b_5 complexes, we assumed that the work done by external forces to enforce complex separation is proportional to the dissociation free energy. SMD calculations nicely show negative values of work for complexes B−E until intermediate distances are reached (Figure 4), which match the observed instabilities of these complexes detected during unconstrained molecular dynamics simulations. The work required to rupture complexes B−E is small, ranging between 0 and 9 kcal/mol, whereas complex A is more cohesive, yielding an apparent dissociation free energy of 26 ± 10 kcal/mol.

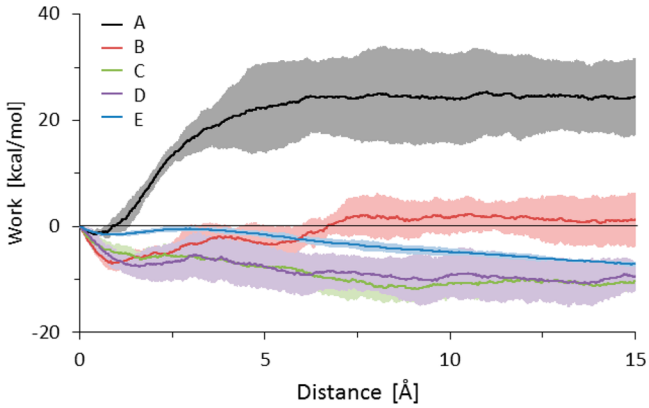

Figure 4. Work done by pulling of cyt b_5 away from P450 1A2 in binding modes A−E calculated using the SMD protocol in an implicit solvent environment. The light belt indicates the standard deviation obtained from three parallel calculations: black for mode A, red for mode B, green for mode C, purple for mode D, and blue for mode E.

Interfacial Electrostatic Complementarity. When the charge states of ionizable protein residues are assigned according to their solution pK_a values, the P450 1A2 and cyt b_5 proteins carry total charges of +11 and −8, respectively. The negative charge of unbound cyt b_5 is localized predominantly in the heme binding domain and partially on propionate groups of heme (Figure 5, top right). In contrast, free P450 1A2 shows the accumulation of positive charges at the bottom part of the contact surface (Figure 5, top left). The comparison of ES properties of isolated versus interacting proteins, which were obtained from the SMD simulation of the best complex (mode A), revealed significant changes in their ES properties induced during their association (Figure 5). When cyt b_5 forms a complex with P450 in model A, its negatively charged heme-binding domain interacts with the positive counterpart on the P450 1A2 surface. Interestingly, the ES complementarity between these proteins already exists before the formation of the complex (ES preorganization effect[81]) and extends upon binding to almost the whole contact surface of complex A (Figure 5, outlined area). P450 1A2 shows a dramatic increase in its ES potential in the contact area during interaction with cyt b_5 (in Figure 5, cf. top left and middle left). In addition, the ES potential at the contact surface of cyt b_5 became more negative during formation of the complex, as the negative part of its ES isosurface is projected further from the cyt b_5 surface (in Figure 5, cf. top right and middle right).

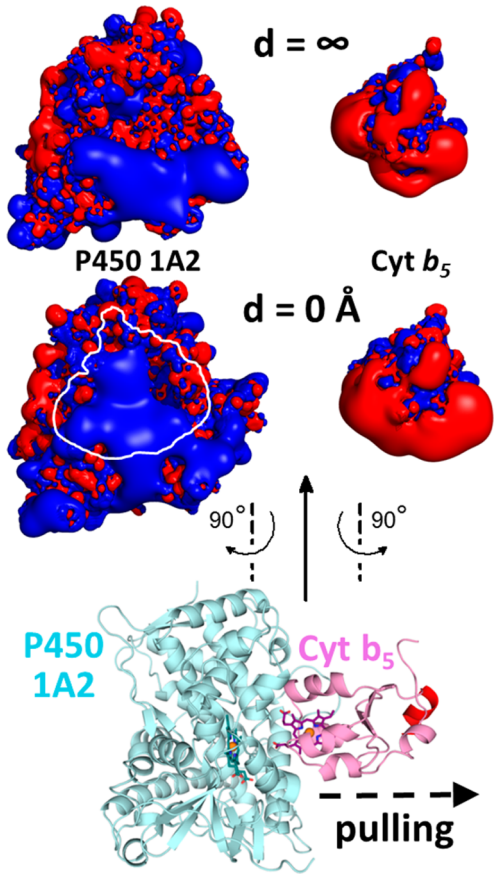

Figure 5. Changes in ES properties of P450 1A2 and cyt b_5 molecules induced during formation of complex A. Properties of isolated P450 1A2 and cyt b_5 molecules (top) are compared with those from MD-optimized complex A (middle). To aid visualization, MD-optimized complex A was disassembled and rotated to expose the interfacial contact. The ES potential around contact areas is shown as an overlap of positive (blue) and negative (red) ES isosurfaces with isovalues set to +2 and −2 k_BT/e, respectively. The resulting complex A is also shown (bottom). The dashed arrow indicates the pulling direction of cyt b_5 that was used during SMD calculations.

Structure of the P450 1A2−Cyt b_5 Complex. Mutual orientation of P450 1A2 and cyt b_5 in the most stable complex (mode A) was not significantly altered during the MD relaxation. For example, the heme−heme distance increased by 0.4 Å, and the interfacial buried surface area of the relaxed P450 1A2−cyt b_5 complex was 1765 Å^2. This value is within the range of buried surface area predicted by docking (1650 ± 150 Å^2). Nevertheless, a majority of the interface was partially hydrated by a discontinuous monomolecular water layer. Major interfacial contacts in this complex involve nine ion pairs between positively charged R95, R100, R138, R362, K442, K455, and K465 side chains of P450 1A2 and negatively charged E42, E43, E49, D65, D71, and heme propionates of cyt b_5. These ion pairs are located at the top, right, and bottom part of the P450 1A2 contact area

dx.doi.org/10.1021/bi500814t | Biochemistry 2014, 53, 6695−6705

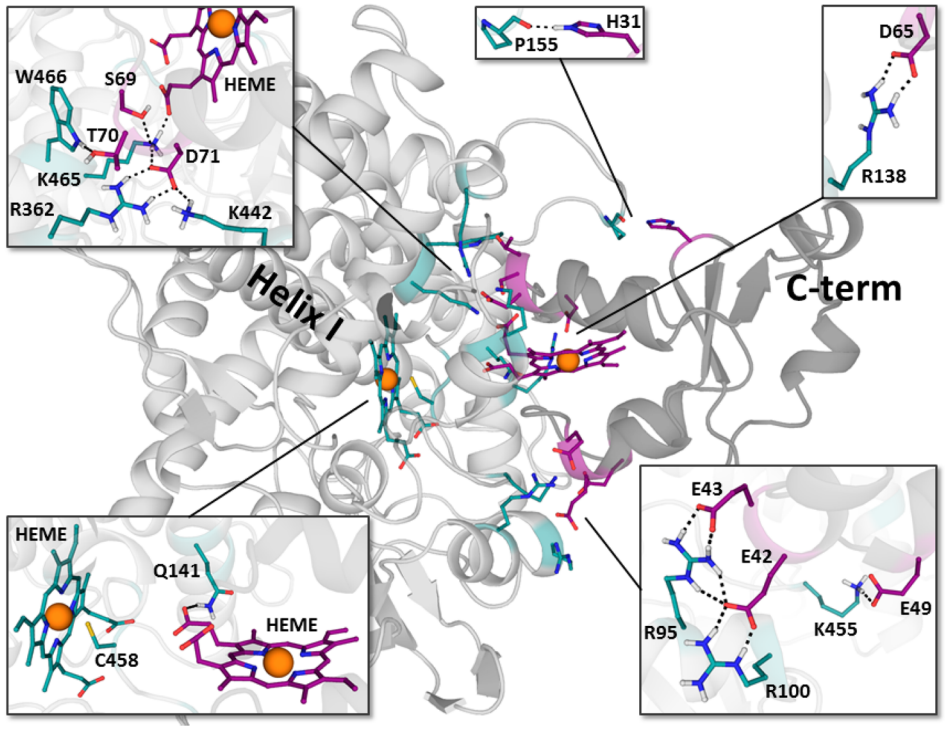

Figure 6. Details of the contact between P450 1A2 and cyt b_5 in MD-optimized binding mode A. The structures were generated from the MD snapshot close to the average over the last nanosecond of the unconstrained MD simulation. The important residues are shown as sticks; Fe^{3+} ions are rendered as orange spheres.

(Figure 6). Positively charged residues of P450 1A2 are located in an area with a highly positive ES potential (Figure 5, middle left). The appearance of the upper part of the positive ES potential induced in P450 1A2 after interaction with cyt b_5 could be associated with rearrangement of residues R362 and K465 (Figure 6), because their basic groups are in the model A shifted outward by 2.3 and 4.5 Å, respectively.

We found no significant interprotein hydrophobic contacts in the resulting complex. The specific protein−protein contacts include four hydrogen bonds between residues Q141, P155, K465, and W466 of P450 1A2 and heme propionates, H31, S69, and T70 of cyt b_5, respectively (Figure 6). Some of these residues (R138, K455, D65, and heme) were already considered important in information-driven protein−protein docking (Table 1), but most of these contacts were established during MD simulations.

DISCUSSION

Several dissimilar complexes of P450 1A2 and cyt b_5 were obtained using information-driven flexible protein−protein docking. We noticed that some experimental information about interacting residues is essential for identifying the most stable complex among the initially docked complexes. The successful experimentally driven constraints included R138, K455, and both heme residues. In contrast, *ab initio* docking failed to produce the most stable complex. The large population of structures generated using experimentally driven constraints highlighted the possible significance of binding mode A (Table 2). However, the scoring and contact data obtained from HADDOCK were inconclusive, showing highest scores for binding modes C and E (Table 2). The classical protein−protein docking procedure is frequently successful in predicting interfaces of proteins showing highly complementary shapes that are already present in monomers prior to the formation of a dimer. However, the medium- and low-affinity complexes are more common in biological systems.[82] Typically, both proteins have to adapt to each other by backbone movement and simultaneously by modifying the conformations of their side chains.[83] Nevertheless, even the incompletely adapted protein−protein binding partners are likely to stay around their binding sites.[84] That is, an ES part of the "preorganization" component is to some extent already present in the nascent binary complex.[81]

Therefore, we aimed to identify and further optimize the best binding mode on a more rigorous basis. Representatives of five binding modes (Figure 1) were reevaluated using two independent techniques of molecular mechanics, MD and SMD. These techniques allowed us to employ more rigorous approximations of ES interactions and a solvent model, thus promising significant improvement over docking. Indeed, mode A (Figure 6), which was the only complex that remained in the vicinity of the initial docked position, was substantially improved as five new interprotein ES contacts were formed during unconstrained MD simulation (Figure 3D). The other binding modes became dissociated during the course of the MD simulations; this behavior indicated a low stability of binding modes B−E. However, there was still the possibility that the initial large-scale structural fluctuation of complexes B−E might revert to the original bound complex, or mode A could start to dissociate on a longer time scale. Therefore, the energetics of the dissociation process was examined using the SMD approach. The overall scheme of our comprehensive modeling strategy is shown in Figure 7.

Results obtained from both MD methods indicate that only mode A of the P450 1A2−cyt b_5 complex is stable. Moreover, the part of the cyt b_5 surface that is participating in the protein−protein interface in this orientation is consistent with the structure of the interface of the distantly homologous P450

dx.doi.org/10.1021/bi500814t | *Biochemistry* 2014, 53, 6695−6705

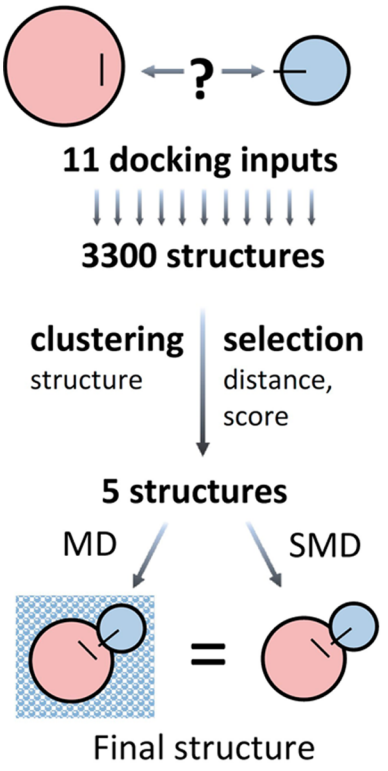

Figure 7. Scheme of our comprehensive modeling strategy. Eleven information-driven flexible docking runs with varying input data evaluated 3300 possible structures. Thirteen proposed complexes (Table 2) showing good scores were regrouped into five superclusters representing structurally distinctive binding modes. Five resulting unique best binding modes were reevaluated by two independent techniques, SMD and MD. Both methods identified the same best binding mode.

3A4−cyt b_5 complex.[85] Finally, the average heme−heme distance of 10.7 Å in this mode could support fast electron transfer between heme cofactors.[74] Thus, we believe that this model could represent a structure that is close to the biologically relevant P450 1A2−cyt b_5 complex.

Zhao et al. also used a homology model of cyt b_5 based on the bovine cyt b_5 to study the P450 3A4−cyt b_5 complex but performed manual docking utilizing information from their own mass spectrometry cross-linking data.[85] The only major difference between the structure of the P450 3A4−cyt b_5 complex and our mode A is the angle β (Figure 2) that differs by approximately 60°. Such small deviations are surprising because the surface residues on P450 3A4 and 1A2 are frequently different. For example, on the basis of our structural alignment of various P450 isoforms, R446 that was found to be important in P450 3A4−cyt b_5 and P450 3A4−NADPH:P450 oxidoreductase complexes[85] is in human P450 1A2 replaced with V462. This variability indicates that the resulting surface shape and interfacial ES properties of both proteins, not individual surface residues, are important for stabilization of P450−cyt b_5 complexes.

This study investigates the mutual interactions of soluble domains of P450 1A2 and cyt b_5 molecules, because three-dimensional structures of their membrane anchors are yet unknown. Fortunately, the improvement in theoretical methods that predict structures of membrane-bound cytochromes P450[86,87] facilitates construction and evaluation of membrane-bound forms of these proteins. The effect of the membrane environment on protein−protein interactions in the P450 1A2−cyt b_5 complex is now a subject of interest for us. However, we believe that this effect would not be dramatic and that the mutual orientation of both proteins will remain similar. According to the spatial arrangement of P450 1A2 in a membrane bilayer predicted in the OPM database [Orientations of Proteins in Membranes (http://opm.phar.umich.edu)], the contact interface of P450 1A2 should be positioned more than 10 Å from the membrane bilayer. In addition to that, the studies comparing the atomistic simulations of the membrane-bound models of cytochromes P450 2C9 and 3A4 with the corresponding models of soluble forms revealed that interaction with a membrane has only limited effects on the overall structure of P450, mainly on the substrate access tunnels on the opposite side of the P450 molecule.[86,87]

For a convenient comparison of various P450−cyt b_5 complexes, a set of six geometrical parameters describing the mutual orientation of two heme molecules was proposed (Figure 2). In addition to a comparison of structures of various P450 complexes, these parameters can facilitate consistent classification of the orientation of the two porphyrins in any protein complexes. We also evaluated the contribution of heme flexibility to fluctuations of geometric parameters introduced here, but only a negligible effect (< 4°) was observed (Table S3 of the Supporting Information). These fluctuations were smaller than dynamic motion of unconstrained proteins in mode A (see SD in Table S3 of the Supporting Information). Tcl script that extracts parameters, which describe the mutual orientation of porphyrin molecules from coordinate files, is provided in the Supporting Information (measurehemes.tcl).

In conclusion, we identified a possible structure of the P450 1A2−cyt b_5 complex. We also proposed that a classical MD and in particular a SMD method could well complement docking of weak, transient protein−protein complexes. This is true especially in cases in which docking results are rather inconclusive, i.e., when several equally probable binding orientations are predicted, or when moderate structural adjustments are necessary to stabilize the resulting complex. Our results might help to elucidate biological roles of the P450 1A2−cyt b_5 complex and improve our understanding of cyt b_5-mediated modulation of P450.

■ ASSOCIATED CONTENT

Supporting Information

Sequence alignment of soluble domains of human and bovine cyt b_5 used for homology modeling, positions of active and passive residues used as restrains for information-driven protein−protein docking, equilibration protocol for MD and SMD simulations, matrix of rmsd values calculated between all structures obtained from protein−protein docking, effects of heme flexibility on the heme-centric internal coordinate system, and Tcl script for the generation of universal heme-centered internal coordinates. This material is available free of charge via the Internet at http://pubs.acs.org.

■ AUTHOR INFORMATION

Corresponding Author

*E-mail: vaclav.martinek@natur.cuni.cz. Phone: (420) 221-951344.

Funding

This work was supported by the Grant Agency of the Czech Republic (Grant 14-18344S in Panel P301) and Charles University (UNCE 204025/2012).

Notes

The authors declare no competing financial interest.

■ ACKNOWLEDGMENTS

Access to the MetaCentrum and CERIT-SC computing facilities provided under Program LM2010005 and CZ.1.05/3.2.00/08.0144 is greatly appreciated.

■ ABBREVIATIONS

P450, cytochrome P450; cyt b_5, cytochrome b_5; MD, molecular dynamics; SMD, steered molecular dynamics; PDB, Protein Data Bank; ES, electrostatic; r_{da}, donor−acceptor distance; rmsd, root-mean-square deviation.

■ REFERENCES

(1) Gonzalez, F. J., and Gelboin, H. V. (1992) Human cytochromes P450: Evolution and cDNA-directed expression. *Environ. Health Perspect. 98*, 81−85.

(2) Finn, R. D., McLaughlin, L. A., Ronseaux, S., Rosewell, I., Houston, J. B., Henderson, C. J., and Wolf, C. R. (2008) Defining the in vivo role for cytochrome b5 in cytochrome P450 function through the conditional hepatic deletion of microsomal cytochrome b5. *J. Biol. Chem. 283*, 31385−31393.

(3) Im, S.-C., and Waskell, L. (2011) The interaction of microsomal cytochrome P450 2B4 with its redox partners, cytochrome P450 reductase and cytochrome b_5. *Arch. Biochem. Biophys. 507*, 144−153.

(4) McLaughlin, L. A., Ronseaux, S., Finn, R. D., Henderson, C. J., and Roland Wolf, C. (2010) Deletion of microsomal cytochrome b5 profoundly affects hepatic and extrahepatic drug metabolism. *Mol. Pharmacol. 78*, 269−278.

(5) Jansson, I., and Schenkman, J. B. (1996) Substrate influence on interaction between cytochrome P450 and cytochrome b5 in microsomes. *Arch. Biochem. Biophys. 325*, 265−269.

(6) Morgan, E. T., and Coon, M. J. (1984) Effects of cytochrome b5 on cytochrome P-450-catalyzed reactions. Studies with manganese-substituted cytochrome b5. *Drug Metab. Dispos. 12*, 358−364.

(7) Gruenke, L. D., Konopka, K., Cadieu, M., and Waskell, L. (1995) The stoichiometry of the cytochrome P-450-catalyzed metabolism of methoxyflurane and benzphetamine in the presence and absence of cytochrome b5. *J. Biol. Chem. 270*, 24707−24718.

(8) Schenkman, J. B., and Jansson, I. (2003) The many roles of cytochrome b5. *Pharmacol. Ther. 97*, 139−152.

(9) Rivera, M., Seetharaman, R., Girdhar, D., Wirtz, M., Zhang, X., Wang, X., and White, S. (1998) The reduction potential of cytochrome b5 is modulated by its exposed heme edge. *Biochemistry 37*, 1485−1494.

(10) Porter, T. D. (2002) The roles of cytochrome b5 in cytochrome P450 reactions. *J. Biochem. Mol. Toxicol. 16*, 311−316.

(11) Zhang, H., Im, S.-C., and Waskell, L. (2007) Cytochrome b5 increases the rate of product formation by cytochrome P450 2B4 and competes with cytochrome P450 reductase for a binding site on cytochrome P450 2B4. *J. Biol. Chem. 282*, 29766−29776.

(12) Yamazaki, H., Johnson, W. W., Ueng, Y. F., Shimada, T., and Guengerich, F. P. (1996) Lack of electron transfer from cytochrome b5 in stimulation of catalytic activities of cytochrome P450 3A4. Characterization of a reconstituted cytochrome P450 3A4/NADPH-cytochrome P450 reductase system and studies with apo-cytochrome b5. *J. Biol. Chem. 271*, 27438−27444.

(13) Yamazaki, H., Shimada, T., Martin, M. V., and Guengerich, F. P. (2001) Stimulation of cytochrome P450 reactions by apo-cytochrome b5: Evidence against transfer of heme from cytochrome P450 3A4 to apo-cytochrome b5 or heme oxygenase. *J. Biol. Chem. 276*, 30885−30891.

(14) Yamazaki, H., Nakamura, M., Komatsu, T., Ohyama, K., Hatanaka, N., Asahi, S., Shimada, N., Guengerich, F. P., Shimada, T., Nakajima, M., and Yokoi, T. (2002) Roles of NADPH-P450 reductase and apo- and holo-cytochrome b5 on xenobiotic oxidations catalyzed by 12 recombinant human cytochrome P450s expressed in membranes of *Escherichia coli*. *Protein Expression Purif. 24*, 329−337.

(15) Kotrbova, V., Aimova, D., Ingr, M., Borek-Dohalska, L., Martinek, V., and Stiborova, M. (2009) Preparation of a biologically active apo-cytochrome b_5 via heterologous expression in *Escherichia coli*. *Protein Expression Purif. 66*, 203−209.

(16) Zhang, H., Hamdane, D., Im, S.-C., and Waskell, L. (2008) Cytochrome b5 inhibits electron transfer from NADPH-cytochrome P450 reductase to ferric cytochrome P450 2B4. *J. Biol. Chem. 283*, 5217−5225.

(17) Stiborová, M., Martínek, V., Schmeiser, H. H., and Frei, E. (2006) Modulation of CYP1A1-mediated oxidation of carcinogenic azo dye Sudan I and its binding to DNA by cytochrome b5. *Neuroendocrinol. Lett. 27* (Suppl. 2), 35−39.

(18) Stiborová, M., Mares, J., Levova, K., Pavlickova, J., Barta, F., Hodek, P., Frei, E., and Schmeiser, H. H. (2011) Role of cytochromes P450 in metabolism of carcinogenic aristolochic acid I: Evidence of their contribution to aristolochic acid I detoxication and activation in rat liver. *Neuroendocrinol. Lett. 32* (Suppl. 1), 121−130.

(19) Kotrbová, V., Mrázová, B., Moserová, M., Martínek, V., Hodek, P., Hudeček, J., Frei, E., and Stiborová, M. (2011) Cytochrome b_5 shifts oxidation of the anticancer drug ellipticine by cytochromes P450 1A1 and 1A2 from its detoxication to activation, thereby modulating its pharmacological efficacy. *Biochem. Pharmacol. 82*, 669−680.

(20) Stiborová, M., Indra, R., Moserová, M., Cerná, V., Rupertová, M., Martínek, V., Eckschlager, T., Kizek, R., and Frei, E. (2012) Cytochrome b5 increases cytochrome P450 3A4-mediated activation of anticancer drug ellipticine to 13-hydroxyellipticine whose covalent binding to DNA is elevated by sulfotransferases and N,O-acetyltransferases. *Chem. Res. Toxicol. 25*, 1075−1085.

(21) Stiborová, M., Poljaková, J., Martínková, E., Ulrichová, J., Simánek, V., Dvořák, Z., and Frei, E. (2012) Ellipticine oxidation and DNA adduct formation in human hepatocytes is catalyzed by human cytochromes P450 and enhanced by cytochrome b_5. *Toxicology 302*, 233−241.

(22) Sulc, M., Jecmen, T., Snajdrova, R., Novak, P., Martinek, V., Hodek, P., Stiborova, M., and Hudecek, J. (2012) Mapping of interaction between cytochrome P450 2B4 and cytochrome b5: The first evidence of two mutual orientations. *Neuroendocrinol. Lett. 33*, 41−47.

(23) Bridges, A., Gruenke, L., Chang, Y. T., Vakser, I. A., Loew, G., and Waskell, L. (1998) Identification of the binding site on cytochrome P450 2B4 for cytochrome b5 and cytochrome P450 reductase. *J. Biol. Chem. 273*, 17036−17049.

(24) Ahuja, S., Jahr, N., Im, S.-C., Vivekanandan, S., Popovych, N., Clair, S. V. L., Huang, R., Soong, R., Xu, J., Yamamoto, K., Nanga, R. P., Bridges, A., Waskell, L., and Ramamoorthy, A. (2013) A Model of the Membrane-bound Cytochrome b5-Cytochrome P450 Complex from NMR and Mutagenesis Data. *J. Biol. Chem. 288*, 22080−22095.

(25) Zhang, H., Myshkin, E., and Waskell, L. (2005) Role of cytochrome b5 in catalysis by cytochrome P450 2B4. *Biochem. Biophys. Res. Commun. 338*, 499−506.

(26) Gao, Q., Doneanu, C. E., Shaffer, S. A., Adman, E. T., Goodlett, D. R., and Nelson, S. D. (2006) Identification of the interactions between cytochrome P450 2E1 and cytochrome b5 by mass spectrometry and site-directed mutagenesis. *J. Biol. Chem. 281*, 20404−20417.

(27) Peng, H.-M., and Auchus, R. J. (2013) The Action of Cytochrome b_5 on CYP2E1 and CYP2C19 Activities Requires Anionic Residues D58 and D65. *Biochemistry 52*, 210−220.

(28) Estrada, D. F., Laurence, J. S., and Scott, E. E. (2013) Substrate-modulated Cytochrome P450 17A1 and Cytochrome b5 Interactions Revealed by NMR. *J. Biol. Chem. 288*, 17008−17018.

(29) Shimada, T., Mernaugh, R. L., and Guengerich, F. P. (2005) Interactions of mammalian cytochrome P450, NADPH-cytochrome P450 reductase, and cytochrome b_5 enzymes. *Arch. Biochem. Biophys. 435*, 207−216.

(30) Dürr, U. H. N., Waskell, L., and Ramamoorthy, A. (2007) The cytochromes P450 and b5 and their reductases: Promising targets for

structural studies by advanced solid-state NMR spectroscopy. *Biochim. Biophys. Acta 1768*, 3235−3259.
(31) Stiborová, M., Martínek, V., Rýdlová, H., Hodek, P., and Frei, E. (2002) Sudan I is a potential carcinogen for humans: Evidence for its metabolic activation and detoxication by human recombinant cytochrome P450 1A1 and liver microsomes. *Cancer Res. 62*, 5678−5684.
(32) Stiborová, M., Martínek, V., Rýdlová, H., Koblas, T., and Hodek, P. (2005) Expression of cytochrome P450 1A1 and its contribution to oxidation of a potential human carcinogen 1-phenylazo-2-naphthol (Sudan I) in human livers. *Cancer Lett. 220*, 145−154.
(33) Stiborová, M., Dracínská, H., Mizerovská, J., Frei, E., Schmeiser, H. H., Hudecek, J., Hodek, P., Phillips, D. H., and Arlt, V. M. (2008) The environmental pollutant and carcinogen 3-nitrobenzanthrone induces cytochrome P450 1A1 and NAD(P)H:quinone oxidoreductase in rat lung and kidney, thereby enhancing its own genotoxicity. *Toxicology 247*, 11−22.
(34) Stiborová, M., Rupertová, M., and Frei, E. (2011) Cytochrome P450- and peroxidase-mediated oxidation of anticancer alkaloid ellipticine dictates its anti-tumor efficiency. *Biochim. Biophys. Acta 1814*, 175−185.
(35) Aimová, D., Svobodová, L., Kotrbová, V., Mrázová, B., Hodek, P., Hudecek, J., Václavíková, R., Frei, E., and Stiborová, M. (2007) The anticancer drug ellipticine is a potent inducer of rat cytochromes P450 1A1 and 1A2, thereby modulating its own metabolism. *Drug Metab. Dispos. 35*, 1926−1934.
(36) Levová, K., Moserová, M., Kotrbová, V., Sulc, M., Henderson, C. J., Wolf, C. R., Phillips, D. H., Frei, E., Schmeiser, H. H., Mares, J., Arlt, V. M., and Stiborová, M. (2011) Role of cytochromes P450 1A1/2 in detoxication and activation of carcinogenic aristolochic acid I: Studies with the hepatic NADPH:cytochrome P450 reductase null (HRN) mouse model. *Toxicol. Sci. 121*, 43−56.
(37) Miksanová, M., Sulc, M., Rýdlová, H., Schmeiser, H. H., Frei, E., and Stiborová, M. (2004) Enzymes involved in the metabolism of the carcinogen 2-nitroanisole: Evidence for its oxidative detoxication by human cytochromes P450. *Chem. Res. Toxicol. 17*, 663−671.
(38) Arlt, V. M., Stiborová, M., Henderson, C. J., Thiemann, M., Frei, E., Aimová, D., Singh, R., Gamboa da Costa, G., Schmitz, O. J., Farmer, P. B., Wolf, C. R., and Phillips, D. H. (2008) Metabolic activation of benzo[a]pyrene in vitro by hepatic cytochrome P450 contrasts with detoxification in vivo: Experiments with hepatic cytochrome P450 reductase null mice. *Carcinogenesis 29*, 656−665.
(39) Stiborová, M., Moserová, M., Černá, V., Indra, R., Dračínský, M., Šulc, M., Henderson, C. J., Wolf, C. R., Schmeiser, H. H., Phillips, D. H., Frei, E., and Arlt, V. M. (2014) Cytochrome b5 and epoxide hydrolase contribute to benzo[a]pyrene-DNA adduct formation catalyzed by cytochrome P450 1A1 under low NADPH:P450 oxidoreductase conditions. *Toxicology 318*, 1−12.
(40) Venkatesan, K., Rual, J.-F., Vazquez, A., Stelzl, U., Lemmens, I., Hirozane-Kishikawa, T., Hao, T., Zenkner, M., Xin, X., Goh, K.-I., Yildirim, M. A., Simonis, N., Heinzmann, K., Gebreab, F., Sahalie, J. M., Cevik, S., Simon, C., de Smet, A.-S., Dann, E., Smolyar, A., Vinayagam, A., Yu, H., Szeto, D., Borick, H., Dricot, A., Klitgord, N., Murray, R. R., Lin, C., Lalowski, M., Timm, J., Rau, K., Boone, C., Braun, P., Cusick, M. E., Roth, F. P., Hill, D. E., Tavernier, J., Wanker, E. E., Barabási, A.-L., and Vidal, M. (2009) An empirical framework for binary interactome mapping. *Nat. Methods 6*, 83−90.
(41) Guo, Q., Jureller, J. E., Warren, J. T., Solomaha, E., Florián, J., and Tang, W.-J. (2008) Protein-Protein Docking and Analysis Reveal That Two Homologous Bacterial Adenylyl Cyclase Toxins Interact with Calmodulin Differently. *J. Biol. Chem. 283*, 23836−23845.
(42) De Vries, S. J., van Dijk, A. D. J., Krzeminski, M., van Dijk, M., Thureau, A., Hsu, V., Wassenaar, T., and Bonvin, A. M. J. J. (2007) HADDOCK versus HADDOCK: New features and performance of HADDOCK2.0 on the CAPRI targets. *Proteins 69*, 726−733.
(43) De Vries, S. J., van Dijk, M., and Bonvin, A. M. J. J. (2010) The HADDOCK web server for data-driven biomolecular docking. *Nat. Protoc. 5*, 883−897.
(44) Pons, C., Grosdidier, S., Solernou, A., Pérez-Cano, L., and Fernández-Recio, J. (2010) Present and future challenges and limitations in protein-protein docking. *Proteins 78*, 95−108.
(45) La, D., Kong, M., Hoffman, W., Choi, Y. I., and Kihara, D. (2013) Predicting permanent and transient protein−protein interfaces. *Proteins: Struct., Funct., Bioinf. 81*, 805−818.
(46) Singh, N., and Warshel, A. (2010) Absolute binding free energy calculations: On the accuracy of computational scoring of protein-ligand interactions. *Proteins 78*, 1705−1723.
(47) Martínek, V., Bren, U., Goodman, M. F., Warshel, A., and Florián, J. (2007) DNA polymerase β catalytic efficiency mirrors the Asn279-dCTP H-bonding strength. *FEBS Lett. 581*, 775−780.
(48) Bren, U., and Oostenbrink, C. (2012) Cytochrome P450 3A4 Inhibition by Ketoconazole: Tackling the Problem of Ligand Cooperativity Using Molecular Dynamics Simulations and Free-Energy Calculations. *J. Chem. Inf. Model. 52*, 1573−1582.
(49) Almlöf, M., Åqvist, J., Smalås, A. O., and Brandsdal, B. O. (2006) Probing the Effect of Point Mutations at Protein-Protein Interfaces with Free Energy Calculations. *Biophys. J. 90*, 433−442.
(50) Cuendet, M. A., and Michielin, O. (2008) Protein-protein interaction investigated by steered molecular dynamics: The TCR-pMHC complex. *Biophys. J. 95*, 3575−3590.
(51) Dryga, A., and Warshel, A. (2010) Renormalizing SMD: The renormalization approach and its use in long time simulations and accelerated PMF calculations of macromolecules. *J. Phys. Chem. B 114*, 12720−12728.
(52) Li, W., Shen, J., Liu, G., Tang, Y., and Hoshino, T. (2011) Exploring coumarin egress channels in human cytochrome P450 2A6 by random acceleration and steered molecular dynamics simulations. *Proteins 79*, 271−281.
(53) Chen, L. Y. (2011) Exploring the free-energy landscapes of biological systems with steered molecular dynamics. *Phys. Chem. Chem. Phys. 13*, 6176−6183.
(54) Sansen, S., Yano, J. K., Reynald, R. L., Schoch, G. A., Griffin, K. J., Stout, C. D., and Johnson, E. F. (2007) Adaptations for the oxidation of polycyclic aromatic hydrocarbons exhibited by the structure of human P450 1A2. *J. Biol. Chem. 282*, 14348−14355.
(55) Nunez, M., Guittet, E., Pompon, D., van Heijenoort, C., and Truan, G. (2010) NMR structure note: Oxidized microsomal human cytochrome b5. *J. Biomol. NMR 47*, 289−295.
(56) Schwede, T., Kopp, J., Guex, N., and Peitsch, M. C. (2003) SWISS-MODEL: An automated protein homology-modeling server. *Nucleic Acids Res. 31*, 3381−3385.
(57) Durley, R. C., and Mathews, F. S. (1996) Refinement and structural analysis of bovine cytochrome b5 at 1.5 Å resolution. *Acta Crystallogr. D52*, 65−76.
(58) Bren, U., Kržan, A., and Mavri, J. (2008) Microwave Catalysis through Rotationally Hot Reactive Species. *J. Phys. Chem. A 112*, 166−171.
(59) Bren, M., Janezic, D., and Bren, U. (2010) Microwave catalysis revisited: An analytical solution. *J. Phys. Chem. A 114*, 4197−4202.
(60) Bren, U., and Janežič, D. (2012) Individual degrees of freedom and the solvation properties of water. *J. Chem. Phys. 137*, 024108.
(61) Vriend, G. (1990) WHAT IF: A molecular modeling and drug design program. *J. Mol. Graphics 8*, 52−56.
(62) Grubmüller, H. (1996) *Solvate*, version 1.0, Ludwig-Maximilians-Universität München, Munich.
(63) Humphrey, W., Dalke, A., and Schulten, K. (1996) VMD: Visual molecular dynamics. *J. Mol. Graphics 14*, 33−38.
(64) Phillips, J. C., Braun, R., Wang, W., Gumbart, J., Tajkhorshid, E., Villa, E., Chipot, C., Skeel, R. D., Kalé, L., and Schulten, K. (2005) Scalable molecular dynamics with NAMD. *J. Comput. Chem. 26*, 1781−1802.
(65) Darden, T., York, D., and Pedersen, L. (1993) Particle mesh Ewald: An N·log(N) method for Ewald sums in large systems. *J. Chem. Phys. 98*, 10089−10092.
(66) Ryckaert, J.-P., Ciccotti, G., and Berendsen, H. J. (1977) Numerical integration of the cartesian equations of motion of a system

with constraints: Molecular dynamics of n-alkanes. *J. Comput. Phys. 23*, 327−341.
(67) MacKerell, A. D., Jr., Bashford, D., Bellott, M., Dunbrack, R. L., Jr., Evanseck, J. D., Field, M. J., Fischer, S., Gao, J., Guo, H., Ha, S., Joseph-McCarthy, D., Kuchnir, L., Kuczera, K., Lau, F. T. K., Mattos, C., Michnick, S., Ngo, T., Nguyen, D. T., Prodhom, B., Reiher, W. E., Roux, B., Schlenkrich, M., Smith, J. C., Stote, R., Straub, J., Watanabe, M., Wiórkiewicz-Kuczera, J., Yin, D., and Karplus, M. (1998) All-Atom Empirical Potential for Molecular Modeling and Dynamics Studies of Proteins. *J. Phys. Chem. B 102*, 3586−3616.
(68) Stone, J. E., Hardy, D. J., Ufimtsev, I. S., and Schulten, K. (2010) GPU-accelerated molecular modeling coming of age. *J. Mol. Graphics Modell. 29*, 116−125.
(69) Israelewitz, B., Gao, M., and Schulten, K. (2001) Steered molecular dynamics and mechanical functions of proteins. *Curr. Opin. Struct. Biol. 11*, 224−230.
(70) Park, S., Khalili-Araghi, F., Tajkhorshid, E., and Schulten, K. (2003) Free energy calculation from steered molecular dynamics simulations using Jarzynski's equality. *J. Chem. Phys. 119*, 3559−3566.
(71) Li, D.-C., and Ji, B.-H. (2012) Free energy calculation of single molecular interaction using Jarzynski's identity method: The case of HIV-1 protease inhibitor system. *Acta Mech. Sin. 28*, 891−903.
(72) Baker, N. A., Sept, D., Joseph, S., Holst, M. J., and McCammon, J. A. (2001) Electrostatics of nanosystems: Application to microtubules and the ribosome. *Proc. Natl. Acad. Sci. U.S.A. 98*, 10037−10041.
(73) *The PyMOL Molecular Graphics System*, version 1.3r1 (2010) Schrödinger, LLC, Portland, OR.
(74) Page, C. C., Moser, C. C., Chen, X., and Dutton, P. L. (1999) Natural engineering principles of electron tunnelling in biological oxidation-reduction. *Nature 402*, 47−52.
(75) Mintseris, J., and Weng, Z. (2005) Structure, function, and evolution of transient and obligate protein-protein interactions. *Proc. Natl. Acad. Sci. U.S.A. 102*, 10930−10935.
(76) Jones, S., and Thornton, J. M. (1996) Principles of protein-protein interactions. *Proc. Natl. Acad. Sci. U.S.A. 93*, 13−20.
(77) Kastritis, P. L., and Bonvin, A. M. J. J. (2013) On the binding affinity of macromolecular interactions: Daring to ask why proteins interact. *J. R. Soc., Interface 10*, 20120835.
(78) Masone, D., Vaca, I. C., de Pons, C., Recio, J. F., and Guallar, V. (2012) H-bond network optimization in protein-protein complexes: Are all-atom force field scores enough? *Proteins 80*, 818−824.
(79) Jarzynski, C. (1997) Equilibrium free-energy differences from nonequilibrium measurements: A master-equation approach. *Phys. Rev. E 56*, 5018−5035.
(80) Park, S., and Schulten, K. (2004) Calculating potentials of mean force from steered molecular dynamics simulations. *J. Chem. Phys. 120*, 5946−5961.
(81) Kamerlin, S. C. L., and Warshel, A. (2010) At the dawn of the 21st century: Is dynamics the missing link for understanding enzyme catalysis? *Proteins 78*, 1339−1375.
(82) Kastritis, P. L., Moal, I. H., Hwang, H., Weng, Z., Bates, P. A., Bonvin, A. M. J. J., and Janin, J. (2011) A structure-based benchmark for protein−protein binding affinity. *Protein Sci. 20*, 482−491.
(83) Pedotti, M., Simonelli, L., Livoti, E., and Varani, L. (2011) Computational docking of antibody-antigen complexes, opportunities and pitfalls illustrated by influenza hemagglutinin. *Int. J. Mol. Sci. 12*, 226−251.
(84) Li, X., Moal, I. H., and Bates, P. A. (2010) Detection and refinement of encounter complexes for protein-protein docking: Taking account of macromolecular crowding. *Proteins 78*, 3189−3196.
(85) Zhao, C., Gao, Q., Roberts, A. G., Shaffer, S. A., Doneanu, C. E., Xue, S., Goodlett, D. R., Nelson, S. D., and Atkins, W. M. (2012) Cross-Linking Mass Spectrometry and Mutagenesis Confirm the Functional Importance of Surface Interactions between CYP3A4 and Holo/Apo Cytochrome b5. *Biochemistry 51*, 9488−9500.
(86) Cojocaru, V., Balali-Mood, K., Sansom, M. S. P., and Wade, R. C. (2011) Structure and dynamics of the membrane-bound cytochrome P450 2C9. *PLoS Comput. Biol. 7*, e1002152.
(87) Lonsdale, R., Rouse, S. L., Sansom, M. S. P., and Mulholland, A. J. (2014) A multiscale approach to modelling drug metabolism by membrane-bound cytochrome P450 enzymes. *PLoS Comput. Biol. 10*, e1003714.